Field behaviour of the XY chiral model on a Cayley tree

1992 J. Phys. A: Math. Gen. 25 1405

(http://iopscience.iop.org/0305-4470/25/6/004)

J. Phys. A: Math. Gen. 25 (1992) 1405–1415. Printed in the UK

Field behaviour of the XY chiral model on a Cayley tree

Américo T Bernardes and Mário J de Oliveira

Instituto de Física, Universidade de São Paulo, Caixa Postal 20516, 01498 São Paulo, Brazil

Received 30 December 1990, in final form 28 October 1991

Abstract. In this paper we present a study of the XY chiral model on a Cayley tree in the presence of an external uniform magnetic field. We calculate the phase diagram at zero temperature from a corresponding 1D mapping. Ferromagnetic, commensurate and incommensurate modulated phases as well as chaotic structures are present in the zero temperature limit. In this case we also obtain a devil's staircase and determine the route to chaos, which is in agreement with Feigenbaum's scenario. For finite temperatures, the phase diagrams are obtained from a 2D mapping. The chaotic behaviour is present only at low temperatures.

1. Introduction

Modulated structures are found in several problems of solid state physics. The modulation arises from a competition between the natural ordering of the order parameter and the order of the underlying lattice [1]. There are many experimental examples in which we observe modulated structures: rare-gas monolayers adsorbed on graphite, liquid crystals, thiourea, etc. Magnetic systems with modulated structures are found in several rare-earth compounds.

Basic models with commensurate and incommensurate modulated phases have been proposed and studied in recent decades, the best known being the ANNNI model [2] and the asymmetric p-state clock model, also called the chiral clock model [3, 4]. In the ANNNI model one has competing nearest- and next-nearest-neighbour interactions (ferro- and anti-ferromagnetic interactions), while in the asymmetric clock model only nearest-neighbour interactions are present. The latter has two different interactions between the sites: a ferromagnetic and a vectorial interaction. The competition between them produces a tendency for the phase angle to have a continuous rotation as a function of position along the direction of modulation. The magnetization is characterized by a continuously varying wavenumber q in the modulation direction while in the ferromagnetic phase q is zero. Thus the parameter q is a good label for the modulated phase.

The XY chiral model arises as a generalization of the p-state clock model. We define plane spins at each site of the lattice with ferromagnetic interactions between spins in the plane and competing interactions in the modulated direction (the z direction). In the present work we also introduce an external uniform magnetic field in the x direction. The XY chiral model in a sinusoidal field was solved by Banerjea and Taylor [5]. Their phase diagram is qualitatively similar to that of the Frenkel-Kontorova model. Yokoi *et al* [6] studied the ground state of the XY chiral model in a magnetic field by using the method of effective potentials. They found ferromagnetic, commensurate and incommensurate phases. In the low-field region their phase diagram

0305-4470/92/061405+11$04.50

is also very similar to that of the Frenkel-Kontorova model, while at high field only the ferromagnetic phase is present.

In this publication we study the XY chiral model in a magnetic field on a Cayley tree in the infinite coordination limit, through a 2D nonlinear mapping. We remark that this limit produces simple equations which are amenable to some detailed numerical investigations. A similar procedure has been used by Yokoi *et al* [7] to obtain the infinite coordination limit of Vannimenus's mapping for an analogue of the ANNNI model on a Cayley tree [8, 9]. The model is solved by a recursion relation which we derive in section 2. This recursion relation is iterated numerically, yielding different types of attractors which characterize the different phases. In section 3 we analyse the zero temperature behaviour of the model and in section 4 we analyse the model for finite temperatures. Finally, in section 5 we present our conclusions.

2. The model and the recursion relations

The XY chiral model in the presence of a magnetic field can be defined by the Hamiltonian

$$\mathcal{H} = -J_1 \sum_{(ij)} \boldsymbol{S}_i \cdot \boldsymbol{S}_j - J_2 \sum_{(ij)} (\boldsymbol{S}_i \times \boldsymbol{S}_j) \cdot \hat{z} - \sum_i \boldsymbol{H} \cdot \boldsymbol{S}_i \tag{1}$$

where the sum (ij) is over nearest neighbours. The spins $\boldsymbol{S}_i$ have components in the xy plane only, and $\hat{z}$ represents the direction of modulation. On a Cayley tree $\hat{z}$ points towards the centre of the tree and the phase modulation takes place with respect to the generations of the tree. We start by considering the p-state chiral model and only later take the limit of an infinite number of states in order to reobtain the continuous vector interactions.

The components of the spin $\boldsymbol{S}_i$ can be written as $S_{i_x} = \cos \varphi_i$ and $S_{i_y} = \sin \varphi_i$, where $\varphi_i = 2\pi n_i / p$ represents the angle between the direction of the plane spin $\boldsymbol{S}_i$ and the x axis and $n_i = 0, 1, \ldots, p-1$. Thus Hamiltonian (1) can be written in the more usual form

$$\mathcal{H} = -J \sum_{(ij)} \cos\left[\frac{2\pi}{p}(n_i - n_j - \Delta)\right] - H \sum_i \cos\left[\frac{2\pi n_i}{p}\right] \tag{2}$$

where $J_1 = J \cos[2\pi\Delta/p]$, $J_2 = J \sin[2\pi\Delta/p]$ and Δ is the 'chiral field'.

As illustrated in figure 1, we consider a tree with coordination number k and branching ratio r ($r = k-1$). On the boundary of the tree—which we call the zeroth

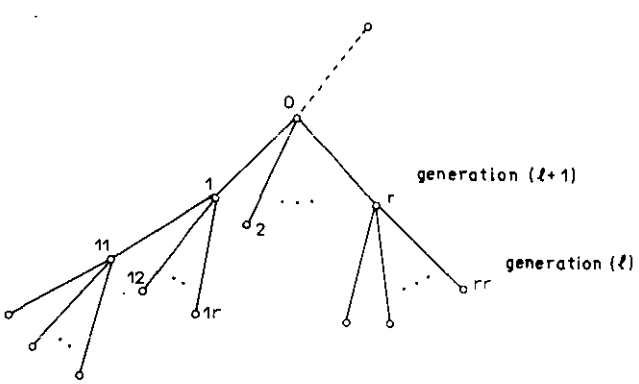

Figure 1. Sub-branch of a Cayley tree with coordination number k (branching ratio $r = k-1$). The site 1 of the generation $(l+1)$ defines the sub-branch.

generation—we fix the states on all sites. The partition function is calculated iteratively by moving from the boundary towards the interior of the tree. The partial partition function of a sub-branch of a generation l where the innermost site i is in state n_i is denoted by $Z_{n_i}(l)$. Then the partial partition functions of the succeeding generations can be related through the expression

$$Z_{n_i}(l+1)=[\exp(-\beta E_{n_i n_j})Z_{n_j}(l)]^r \exp(\beta H \cos\varphi_i) \tag{3}$$

for all $n_i = 0, 1, \ldots, p-1$ with $\beta = 1/k_B T$; where

$$E_{n_i n_j} = -J \cos\left[\frac{2\pi}{p}(n_i - n_j - \Delta)\right] \tag{4}$$

represents the interaction energy between succeeding sites i and j on the Cayley tree.

In the infinite coordination limit ($r \to \infty$) we replace the coupling constant J by J/r as a normalizing condition [10]. In this case we can write

$$\lim_{r\to\infty}\left[\sum_{n_j}\exp(-\beta E_{n_i n_j})Z_{n_j}(l)\Big/\sum_{n_k}Z_{n_k}(l)\right]^r = \exp\left[-\beta\sum_{n_j}E_{n_i n_j}Z_{n_i}(l)\Big/\sum_{n_k}Z_{n_k}(l)\right]. \tag{5}$$

Thus the magnetization of a site i of generation $(l+1)$ may be related to the magnetization of the previous generation l. As we assume uniform boundary conditions, all sites of a generation have the same magnetization. We then use m and m' to represent the magnetizations of successive generations. Recursion relations for the XY chiral model can be obtained by taking the limit of an infinite number of states. For $p \to \infty$, we replace the sum over states, $1/p\,\Sigma_n f[2\pi n/p]$, by the integral $1/2\pi \int f(\theta)\,d\theta$, where $\theta = 2\pi n/p$. Defining the complex magnetization $m = M\,e^{i\varphi}$, where M is the modulus of the magnetization and φ the angle between m and the x axis, we obtain the 2D mapping $M \to M'$, $\varphi \to \varphi'$, given by

$$M' = \frac{I_1(\beta JR)}{I_0(\beta JR)} \tag{6}$$

and

$$\tan\varphi' = \frac{M\sin(\varphi+\delta)}{h + M\cos(\varphi+\delta)} \tag{7}$$

where $R = (h^2 + M^2 + 2hM\cos(\varphi+\delta))$ with $h = H/J$, $\delta = 2\pi\Delta$ and $I_0(x)$ and $I_1(x)$ are the first-class Bessel's functions of order 0 and 1 respectively.

The different phases of the model are now characterized by the different fixed points and periodic orbits of the 2D mapping $(M, \varphi) \to (M', \varphi')$. Five types of attractors are found:

(i) a trivial fixed point which characterizes the paramagnetic phase;

(ii) a non-trivial fixed point which corresponds to the ferromagnetic phase;

(iii) a periodic orbit of period N which corresponds to the commensurate modulated phase of period N;

(iv) a 1D orbit which characterizes the incommensurate modulated phase; and

(v) a strange attractor which characterizes a chaotic structure.

In the following sections we present our results for the phase diagrams of the model.

3. The zero temperature limit

To obtain the equations of the mapping for the zero temperature limit we take the $T=0$ limit in equations (6) and (7). In this case, the magnetization tends to 1, independently of the other variables. The mapping reduces to one dimension and is given by the following equation:

$$\tan\varphi' = \frac{\sin(\varphi+\delta)}{h+\cos(\varphi+\delta)} \tag{8}$$

where φ is the angle between the local magnetization and the x direction. It is easy to see that the phase diagram does not change if Δ is translated by an integer. Also, the phase diagram has reflexive symmetry with respect to the lines $\Delta = 0, \pm 1/2, \pm 1, \pm 3/2, \ldots$. Thus we present the phase diagram for the region $0 \leqslant \Delta \leqslant 0.5$ only.

In order to determine the phase of each point of the phase diagram one must compute the sequence $\varphi_0 \to \varphi_1 \to \varphi_2 \to \ldots$ for arbitrary values of φ_0. The phase is then defined by the winding number

$$q = \lim_{L\to\infty} \frac{1}{2\pi L} \sum_{n=0}^{L} [\tilde{\varphi}_{n+1} - \tilde{\varphi}_n] \tag{9}$$

where $\tilde{\varphi}_{n+1} = \varphi_{n+1}$ if $\varphi_{n+1} > \varphi_n$ or $\tilde{\varphi}_{n+1} = \varphi_{n+1} + 2\pi$ if $\varphi_{n+1} < \varphi_n$.

When $q = 0$ the system is in a ferromagnetic phase. This corresponds to parallel orientation of the spins. A second type of solution corresponds to the case in which the winding number is given by $q = Q/P$, where Q and P are integers. In this case, the system is in a commensurate modulated phase and the winding number coincides with the wavenumber of the helix described by the orientation of successive spins (1). The number Q is the period of the oscillation (rotation of successive spins in the plane perpendicular to the direction of modulation). In a period the spins describe P complete rotations about the direction of modulation.

Finally, in a third type of solution, q may be an irrational number. The system may then be in either of two situations: in an incommensurate modulated phase or in a chaotic phase. The chaotic phase is determined from its Lyapunov exponent [11].

The phase diagram is shown in figure 2. The grey region represents the ferromagnetic phase (which is present in the zero temperature limit only). This region is bounded by the line F. The fixed point which represents the ferromagnetic phase is unstable on this line. If one increases Δ at a constant value of the magnetic field h a 1D orbit arises. This corresponds to a ferromagnetic-modulated second-order phase transition. For $2 < h$, only the ferromagnetic phase is present.

3.1. $h = 0$

For $h = 0$ the mapping reduces to $\varphi' = \varphi + \delta$. Each commensurate modulated phase corresponds to a point on the line $h = 0$. These points form a zero-measure Cantor set [12]. Between any two points which represent commensurate modulated phases, we can find an infinite number of points representing incommensurate modulated phases.

3.2. $0 < h < 1$

If we increase the magnetic field from a point which represents a commensurate modulated phase on the $h = 0$ line, a wedge-shaped region appears in which the system

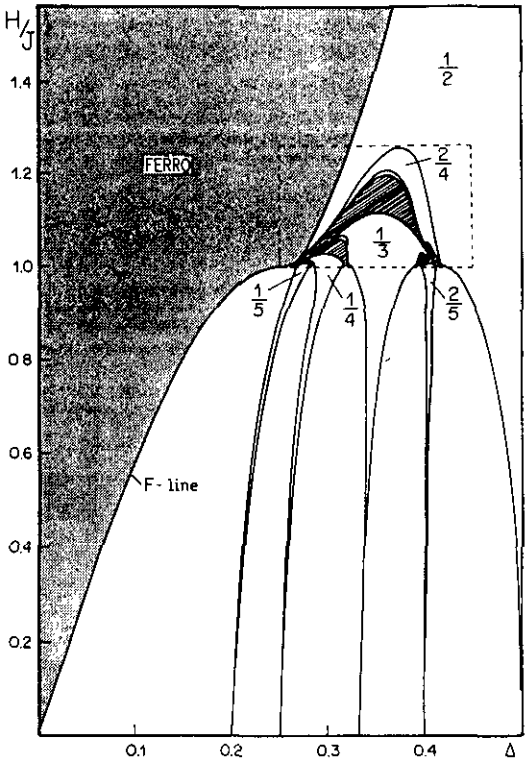

Figure 2. Phase diagram for the zero temperature limit of the XY chiral model (for symmetry reasons we show only the diagram for $0 \leq \Delta \leq 0.5$—see the text). The grey region represents the ferromagnetic phase and the hatched region represents the chaotic phase. The fractional numbers indicate the value of q of the commensurate modulated phases shown in this representation (only five tongues are shown). The dashed rectangle will be amplified in figure 4.

is in the same commensurate modulated phase. These regions are called 'Arnold tongues' [11, 13]. For every rational value of Δ in the $h = 0$ line we obtain a region of a commensurate modulated phase. In the name of clarity, only five of these tongues (1/5, 1/4, 1/3, 2/5 and 1/2) are shown in the figure. The phase 1/2 is the antiferromagnetic phase. Tongues with the same Q (which represent phases with the same period) have the same width. For all phases this width grows when we increase the magnetic field. This growth is associated with the tendency for synchronization of driven oscillations.

As can be seen from figure 2, if we increase Δ at a constant value of the magnetic field, q also increases. If we represent q as a function of Δ, a staircase shape arises, as shown in figure 3. Each step of this staircase corresponds to the width of a commensurate modulated phase. If between two steps we can find an infinite number of steps, this staircase is called a 'devil's staircase' [12]. Each incommensurate modulated phase is only a point in this staircase. If the sum of the widths of the steps is less than the width of the whole interval the staircase is called incomplete (the rational numbers do not occupy the whole space). In this case there are always incommensurate modulated phases between any two commensurate modulated phases. In contrast, if this sum is equal to the interval the staircase is called complete.

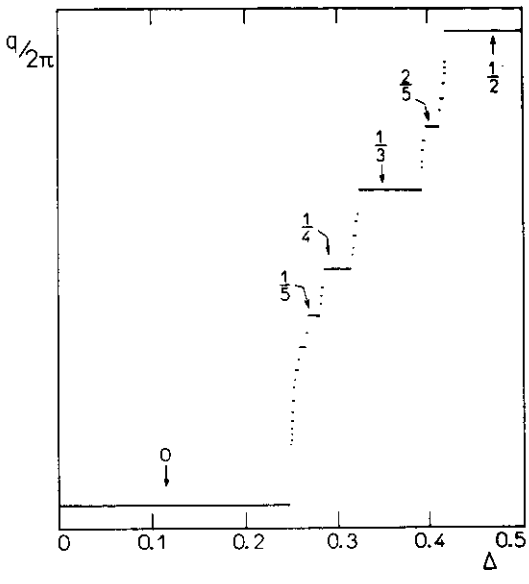

Figure 3. Devil's staircase for the zero temperature limit of the XY chiral model for $h = 1$. We show only the steps with width greater than 10^{-4} (in Δ units).

When h tends to $h = 1$ the commensurate modulated phases tend to dominate the phase space. We show the devil's staircase for $h = 1$ in figure 3 (in this figure we show only the steps with widths greater than 10^{-4} in units of Δ). In order to check whether the staircase is complete, we must calculate the sum of the widths of the steps. The total width was obtained numerically by successively adding up widths greater than $10^{-2}\,\Delta$ units, then widths in the interval $(10^{-2}, 10^{-3})$, and so on, up to widths in the interval $(10^{-7}, 10^{-8})$, as shown in table 1. In particular, the step which corresponds to the ferromagnetic phase contributes with $0.25\,\Delta$ units to the sum. The numerical evidence is that the staircase is complete for $h = 1$.

We note the presence of an inflection point on the F line at $(h = 1, \Delta = 0.25)$. All the boundary lines of the commensurate modulated phases converge to this point (as can be seen in the amplification of the region in the dashed rectangle, figure 4). This

Table 1. Sum of the widths of the incommensurate modulated phases for $h = 1$ in Δ units (for $0 \leq \Delta \leq 0.5$). The width of the ferromagnetic phase (0.25) is included in the sum. The table begins with the phases whose widths are greater than 0.01 and ends with those whose widths are greater than 10^{-8}; 99 phases were included in the summation.

Steps with width greater than:	No. of phases	Sum of widths
10^{-2}	5	0.470 353 480
10^{-3}	11	0.494 022 494
10^{-4}	23	0.499 400 941
10^{-5}	36	0.499 919 791
10^{-6}	51	0.499 986 463
10^{-7}	75	0.499 998 484
10^{-8}	99	0.499 999 131

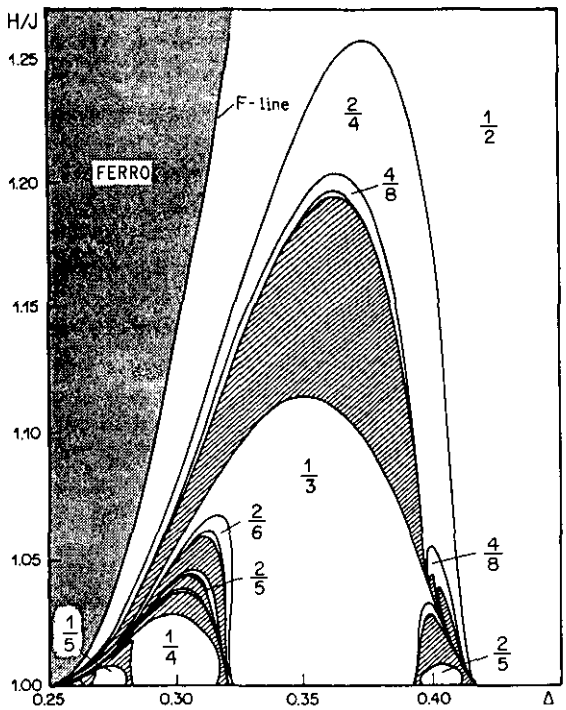

Figure 4. Amplification of the dashed rectangle of the phase diagram shown in figure 2. We observe bifurcations of phases 1/2 and 1/3. We also observe windows in the chaotic region (the phase 2/5 between the phases 1/3 and 1/4 at the bottom and left of the diagram, for instance). All the boundary lines of the commensurate modulated regions converge to the superdegenerate point ($h = 1$, $\Delta = 0.25$).

point also appears in the work of Yokoi *et al* [6], who called it the superdegenerate point. Our phase diagram is similar to theirs.

3.3. $1 < h < 2$

For the above values of the magnetic field the tongues which represent the commensurate modulated phases may overlap. The chaotic phase emerges from this tendency. In analytical results as well as in Monte Carlo calculations, there is always a stable phase with less free energy than the others [6]. The chaotic phase at $T = 0$ is a mathematical possibility of the mapping equation which is also observed in the analysis of the van der Pol driving oscillator [14].

Thus, in this region, both commensurate modulated phases and chaotic phases are observed. The order parameter q has a behaviour quite different from that of the previous region. A change in one parameter (h or Δ) or both can make the system unstable and give rise to a bifurcation. There appears a new phase with the same q but with double period, as can be seen in figure 4. The phase 1/2 bifurcates to 2/4, which in turn bifurcates to 4/8, etc.

The value of the Lyapunov exponent defines the point of bifurcation. We obtained the widths of the phases and the branch splittings in the phase space in a process of successive bifurcations and computed Feigenbaum's coefficients (δ and α) from the

relations

$$\delta_i = \frac{d_i - d_{i-1}}{d_{i+1} - d_i} \tag{10a}$$

and

$$\alpha_j = \frac{\varepsilon_j}{\varepsilon_{j+1}} \tag{10b}$$

where d_i is the width of the ith phase and ε_j is the branch splitting for the jth bifurcation. In table 2 we present the results of our calculations for $h = 1.19$ and varying Δ (we have calculated these parameters with a precision of 10^{-10} for δ and 10^{-6} for α. We spent 60 hours of CPU time on a C220 Convex computer). We give some numerical evidence to show that this coefficient converges to Feigenbaum's coefficient and we thus have a route to chaos in agreement with Feigenbaum's scenario. In our diagram we also find windows inside the chaotic region, as in Feigenbaum's work. These windows have their bifurcations as well.

Table 2. Feigenbaum's coefficients (δ_i and α_j, see text) computed for $h = 1.19$, from the antiferromagnetic phase up to the 256/512 phase for δ and 512/1024 phase for α.

	Feigenbaum's coefficients	
Phase	δ_i	α_j
2/4	2.222	1.070
4/8	2.664	3.306
8/16	3.504	2.057
16/32	4.234	2.684
32/64	4.559	2.431
64/128	4.644	2.539
128/256	4.664	2.490
256/512		2.527

4. Phase diagrams for $T > 0$

We have obtained phase diagrams for $T = 0.03$ (figure 5) and $T = 0.2$ (figure 6) from the mapping equations (6) and (7). For $T > 0.5$ only the paramagnetic phase is present. For temperatures near $T = 0$ (see figure 5) the system shows the same regions obtained for the zero temperature behaviour, but with different features. The ferromagnetic phase is replaced by a paramagnetic phase bounded by the P-line.

We also find a region where both the incommensurate and commensurate modulated phases are present and q is an increasing function of Δ. But in this case we cannot define a value of h which limits this region (in the zero temperature limit $h = 1$ limits the region where q is increasing). For values of $h < 0.8$, we have the same features of the zero temperature limit: the tongues which represent the commensurate modulated phases and, between them, incommensurate modulated phases. In this case the tongues are narrower than in the zero temperature case. Again, we show only five of the phases

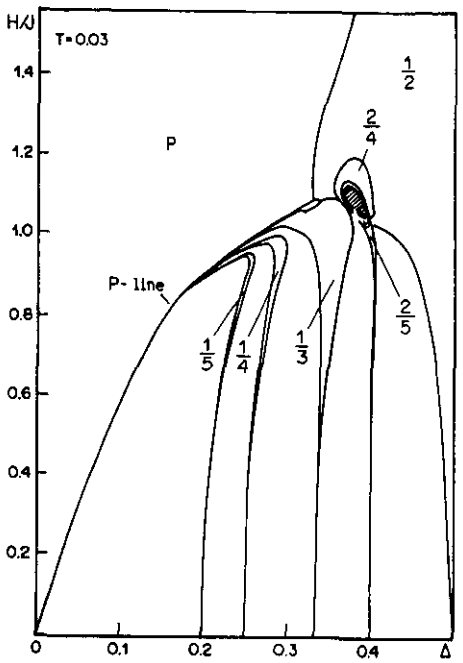

Figure 5. Phase diagram for the XY chiral model calculated for $T = 0.03$. P represents the paramagnetic phase region and the hatched region represents the chaotic region. The fractional numbers indicate the commensurate modulated phases. We also indicate the first bifurcation of the antiferromagnetic phase.

in the phase diagram. For $h > 0.8$ the tongues fold up to meet the P-line. For $h > 1$ we find a chaotic phase and commensurate modulated phases, which bifurcate in the same way as described for the zero temperature limit.

In the phase diagram which represents the system at $T = 0.2$ (figure 6) we find only the paramagnetic, incommensurate and commensurate modulated phases. The modulated regions grow narrower and fold up to meet the P-line, as in the $T = 0.03$ phase diagram. The P-line can be divided into two parts: the first one represents the paramagnetic-commensurate modulated phase transition (with period greater than 2), and the second part represents the paramagnetic-antiferromagnetic transition.

Finally, we show the paramagnetic-modulated phase transition surface (figure 7). On this surface we can observe lines which represent boundaries of the commensurate modulated phases (we show only the lines 1/4, 1/3, 2/5 and 1/2—here called the *AF-M* line). All these lines converge to the superdegenerate point (described in section 3). Here we can clearly see that the two parts of the P-line found in the $T = 0.2$ phase diagram correspond to the two parts of the transition surface, which determine the *AF-M* line.

5. Conclusions

We have presented a solution for the XY chiral model, in a uniform magnetic field, defined on a Cayley tree in the infinite coordination limit. The phases of the system correspond to the attractors of the mapping. In the zero temperature limit the system

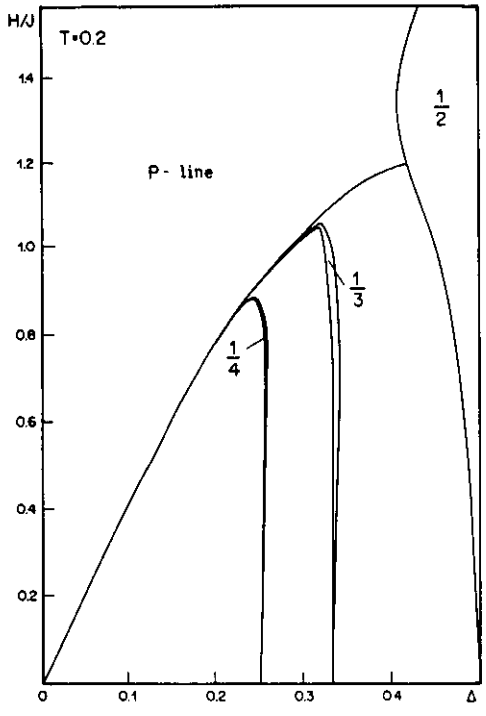

Figure 6. Phase diagram for the XY chiral model calculated for $T = 0.2$. The commensurate modulated regions grow narrower. Here one can see the two parts of the P-line (see text).

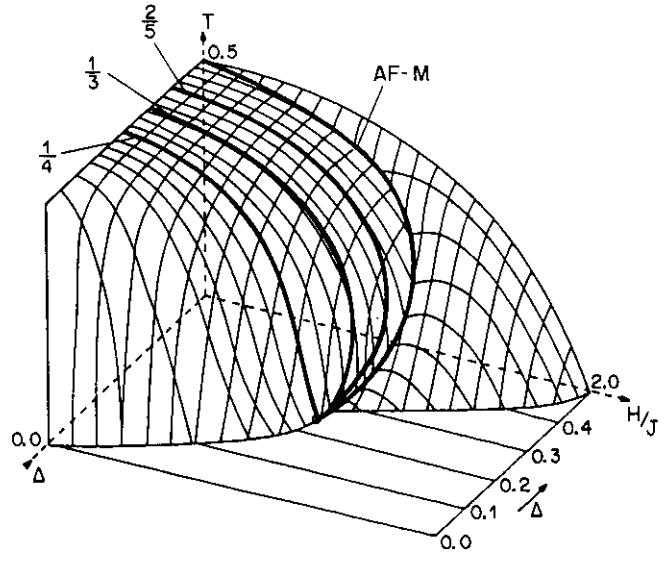

Figure 7. Transition surface between the paramagnetic phase and the modulated phases for the XY chiral model. The lines which represent the boundaries of the commensurate modulated regions (1/4, 1/3, 2/5 and AF-M) are shown. The lines converge to the superdegenerate point. The surface has two parts (see text).

shows commensurate and incommensurate modulated phases and chaotic phases. The chaotic structures arise from the tendency of the commensurate modulated phases to overlap. We have observed a chaotic behaviour as proposed by Jensen *et al* in the general analysis of dissipative systems [15]. The system shows chaotic behaviour only for low temperatures and in the zero temperature limit. The route to chaos seems defined by the scenario of Feigenbaum.

We obtain the phase transition surface in T-h-Δ space. This surface shows two distinct parts. The first separates the antiferromagnetic phase (with $q = 1/2$) from the paramagnetic phase. The second separates the other modulated phases (commensurate or not) from the paramagnetic phase. In this part of the surface we calculate the boundary lines of the commensurate modulated regions below the phase transition surface. In the zero temperature case we also obtain a superdegenerate point at $h = 1$, $\Delta = 0.25$. As we have pointed out above, the superdegenerate point was obtained by Yokoi *et al* for the $T = 0$ case. In our case all these transition lines (for $T = 0$ or $T > 0$) converge to this point.

This work provides a good example of a model displaying many modulated phases. We emphasize the importance of the solution on a Cayley tree, which has allowed us to perform a detailed study of the XY chiral model. The general features of this solution are in agreement with other results. It is not clear, however, whether the existence of a region with a chaotic regime is due to the structure of the tree. This suggests the need for a more thorough study of models with modulated structures on trees and real lattices.

Acknowledgments

We acknowledge fruitful discussions and suggestions from Carlos S O Yokoi, Silvio R Salinas and Vera B Henriques. The work was partially supported by the Brazilian agencies CNPq and CAPES/PICD-UFG.

References

[1] Bak P 1982 *Rep. Prog. Phys.* **45** 587
[2] Elliot R J 1961 *Phys. Rev.* **124** 346
[3] Ostlund S 1981 *Phys. Rev.* B **24** 398
[4] Huse D A 1981 *Phys. Rev.* B **24** 5180
[5] Banerjea A and Taylor P L 1984 *Phys. Rev.* B **30** 6489
[6] Yokoi C S O, Tang L H and Chou W 1988 *Phys. Rev.* B **37** 2173
[7] Yokoi C S O, de Oliveira M J and Salinas S R 1985 *Phys. Rev. Lett.* **54** 163
[8] Vannimenus J 1981 *Z. Phys.* B **43** 141
[9] Inawashiro S, Thompson C J and Honda G 1983 *J. Stat. Phys.* **33** 419
[10] Thompson C J 1982 *J. Stat. Phys.* **27** 441
[11] McCaulley J L 1988 *Phys. Scr.* **T20** 1
[12] Mandelbrot B B 1977 *Fractals: Form, Chance and Dimension* (San Francisco: Freeman)
[13] Arnold V 1985 *Equações Diferenciais Ordinárias* (Moscow: Ed Mir)
[14] Ding E J 1988 *Phys. Scr.* **38** 9
[15] Jensen M H, Bak P and Bohr T 1984 *Phys. Rev.* A **30** 1960